Aljeldah et al | Article 9222
J Pure Appl Microbiol. 2024;18(2):1305-1318. doi: 10.22207/JPAM.18.2.51
Received: 02 January 2024 | Accepted: 02 May 2024
Published Online: 02 June 2024

P-ISSN: 0973-7510; E-ISSN: 2581-690X

RESEARCH ARTICLE OPEN ACCESS

Parasporins of *Bacillus thuringiensis* Strain Exhibit Apoptosis-Mediated Selective Cytotoxicity to MDA-MB-231 Cells through Oxidative Stress

Mohmmed M. Aljeldah[1]*, Talat A. El-kersh[2,3] and Mourad A.M. Aboul-Soud[2]*

[1]Department of Clinical Laboratory Sciences, College of Applied Medical Sciences, University of Hafr Al Batin, Hafr Al Batin 31991, Saudi Arabia.
[2]Department of Clinical Laboratory Sciences, College of Applied Medical Sciences, King Saud University, P.O. Box 10219, Riyadh 11433, Saudi Arabia.
[3]Department of Microbiology & Immunology, School of Pharmacy, Badr University in Cairo (BUC), Badr City, Cairo 11829, Egypt.

Abstract

Historically, the most important source of both antibiotics and anticancer medications has been microorganisms. *Bacillus thuringiensis* (*Bt*) is one of the most prominent bacterial species used as a therapeutic agent targeting cancerous cells in recent worldwide investigations. This study was designed to isolate, molecularly identify, and discover novel Saudi Arabian *Bt* strains that selectively exhibit cytotoxic properties against MDA-MB-231, a human triple-negative breast cancer (TNBC) cell model. The bacterial strain under investigation was biochemically typed using API 20E and API CH50 and molecularly typed using *16S* rDNA sequencing. Flow cytometry and immunoblotting were performed to elucidate the mechanism-of-action (MOA). Molecular typing confirmed the identity of the isolated non-hemolytic strain to be *Bt* and was named *Bt* HAU-145. Microscopic examination showed that the strain possessed a parasporal (PS) crystal protein with a spherical morphology. Data of cytotoxicity assay based on MTT revealed that *Bt* HAU-145 strain exhibited selective and potent cytotoxicity against MDA-MB-231, with a 50 percent inhibition (IC_{50}) of 28 µg/ml. FACS analysis revealed that PS proteins induced both late and early apoptosis in a ROS-dependent manner. Immunoblotting assays showed increased expression of caspase-3 in response to PS treatment, paralleled by a reduction in Bcl-2 expression. This is the first study to investigate the MOA of PS proteins from the Saudi Arabian *Bt* strain, showing an induction of apoptosis through a ROS-dependent mechanism in TNBC cells. It is hoped that PS-based therapeutic strategies will be investigated at the preclinical scale in non-human primates prior to the clinical scale in randomized clinical trials.

Keywords: *Bacillus thuringiensis*, Apoptosis, Anticancer, Non-insecticidal Inclusions, Parasporins, Reactive Oxygen Species

***Correspondence:** mmaljeldah@uhb.edu.sa; maboulsoud@ksu.edu.sa

Citation: Aljeldah MM, El-kersh TA, Aboul-Soud MAM. Parasporins of *Bacillus thuringiensis* Strain Exhibit Apoptosis-Mediated Selective Cytotoxicity to MDA-MB-231 Cells through Oxidative Stress. *J Pure Appl Microbiol.* 2024;18(2):1305-1318. doi: 10.22207/JPAM.18.2.51

INTRODUCTION

Cancer is a critical global public health issue because it is one of the primary causes of mortality worldwide. In 2020, the worldwide cancer incidence increased dramatically, recording 20 million cases with new diagnosis and 9.7 million fatalities compared to only 12.4 and 7.6 million in 2008, respectively. These rates are expected to climb to an astonishing 26.4 million newly diagnosed cases and a total of 17 million fatalities caused by cancer by 2030.[1] The Saudi Cancer Registry (SCR) is responsible for updating records and registering cancer cases across various regions of the Kingdom. In 2020, the number of newly diagnosed cancer cases and mortalities were 27885 and 13069 cases in KSA, respectively.[2] As a result, KSA and other countries should be ready to tackle the issue of an imminent rise in cancer burden due to increasing risk factors, including obesity, genetic predisposition, changes in lifestyle, smoking, and other environmental factors.[3] Of note, TNBC that lack the estrogen receptor (ER), progesterone receptor (PR), and human epidermal growth factor-receptor 2 (HER2), are immensely aggressive tumors, representing 15–20% of all diagnosed BCs with the poorest prognosis.[4] Moreover, TNBC possesses a unique capacity to evade apoptosis, leading to immortality, which aggravates its insensitivity to chemotherapy.[5] These projected increasing trends in cancer cases and fatalities necessitate preventive measures, early detection techniques, and innovative therapeutic methods. This has spurred the pursuit of natural remedies as alternatives to systemic chemotherapy that would lessen the clinical consequences of TNBC and exhibit a wider safety margin. Therefore, it is critical to discover a novel category of anticancer drugs of natural origin with low toxicity, high selectivity, and the ability to overcome the effects of drug resistance.[6-10]

In this context, some natural bioactive small peptides (5–50 amino acids) have been reported to exhibit powerful anticancer activities through either mitochondrial disruption or membranolytic mechanisms.[11] Some of these ubiquitous short peptides, including Moricin, Brevinin 2R, Bufforin IIb, Phylloseptin-PHa, D-K6L9, are cytotoxic against breast cancer (BC) cells.[11,12] Owing to their remarkable ability to trigger cancer cell death, several of these peptides have been utilized as chemotherapeutic drugs and vaccines and have been tested in various stages of clinical trials.[11]

Historically, microorganisms have been the most important sources of antibiotics and anticancer medications. Non-insecticidal and non-hemolytic *Bacillus thuringiensis* strains have been reported to exert cytotoxic effects against human cancer cells.[13] This potent cytotoxicity is attributed to parasporin (PS), a novel parasporal protein.[13,14] PS was first identified as a human leukemic cell-recognizing PS protein.[13] PS protein are excellent natural anticancer therapeutic agents, which is attributed to its reported selectivity for cancerous cells, with minimal or negligible effects on non-cancerous cells.[15] From this perspective, a recent study of Saudi Arabian *Bt* strains by our group reported the selectivity of PS proteins towards HeLa cervical cancer cells with a marginal effect against non-cancerous uterine smooth muscle cells.[15] Moreover, this observed cytotoxic effect has been reported to be specific to HeLa cells, but not to HT-29 colon cancer cells.[15] Another study reported that *Bt* strains native to the Makkah Province (Saudi Arabia) exerted cytotoxic effects against liver, lung, and cervical cancer cells.[16] Hence, PS proteins offer great promise as a natural and effective alternative therapeutic strategy to currently employed chemotherapeutic drugs, which are based on synthetic drugs with uncontrollable side effects and issues of non-target specificity. The discovery of PS proteins as anticancer agents dates back more than two centuries.[13,14] Nonetheless, a wide gap exists in the knowledge regarding the molecular mechanisms of action of these ubiquitous proteins. This is supported by a limited number of reports on the selectivity of PS proteins against non-cancerous cells.[15]

Because of their ubiquity and remarkable specificity against cancer cells, PS proteins are promising candidates for cancer therapies.[15] As a continuation of our endeavors, the current study was initiated to investigate the anticancer effect of a *Bt* strain isolated from the Hafr Al-Batin region of Saudi Arabia and to dissect its mode of action using flow cytometry and immunoblotting techniques. The model cell line investigated in the current study was MDA-MB-231, which is

classified as a triple-negative subtype of breast cancer (BC) owing to the absence of two hormonal receptors *vis-a-vis* estrogen and progesterone, as well as the amplification of HER-2/Neu markers.[4] This subtype of breast cancer is particularly problematic because of its unfavorable outcome and aggressiveness.[17] Therefore, the current study focused on this specific subtype. To the best of our knowledge, this is the first report from Saudi Arabia investigating the mode of action of PS proteins against this particular BC subtype.

MATERIALS AND METHODS

Isolation of *B. thuringiensis*

Five separate locations in the city of Hafr Al-Batin (Saudi Arabia) were used to recover soil samples containing *B. thuringiensis* (*Bt)* isolates between January and March 2022. Detailed isolation and culturing procedures were performed according to previously published protocols.[18] The strain investigated in this study is hereafter referred to as HAU-145.

Cell lines and culturing protocol

MDA-MB-231 (a triple negative BC cell model; ATCC HTB-26) and MCF-12 (a normal epithelial BC model; ATCC CRL-10782) were obtained from the American Type Culture Collection (ATCC), a bioresource non-profit center that distributes cell lines. The cells were routinely sub-cultured in high-glucose Dulbecco's modified Eagle's medium (DMEM) supplemented with fetal bovine serum (FBS, 10%), L-glutamine (2 mM), and penicillin/streptomycin (1%). Flasks containing cells were incubated at 37°C in a humidified atmosphere for CO_2 and O_2 5% and 95%, respectively. The cultured cells were inspected regularly using an inverted microscope (Observer A1; Zeiss, Gottingen, Germany).

Biochemical typing of *HAU-145* strain

Biochemical characterization of the *Bt* strain was conducted by examining its metabolic activity using a matrix of test results produced by both API 20E and API CH50.[19]

Microscopic examination

Samples were prepared from *Bt* HAU-145 colonies grown at 30°C on nutrient agar for one week. Morphology of crystal-spore complexes that had been air-dried on micro cover glasses was examined by use of scanning electron microscope (Model JSM-6380 LA, Japan) and the associated software (Smile Shot), at 15 kV voltage and 4,300 magnification. Phase-contrast microscopy was conducted using an Olympus CX41 microscope (Olympus Life Sciences, Tokyo, Japan).

Genomic DNA extraction and *16S* rDNA sequencing of *Bt* HAU-145 strain

Genomic DNA of *Bt* HAU-145 strains was rapidly extracted by use of InstaGene Matrix (Bio-Rad, Melville, NY, USA) containing 6% w/v Chelex resin, according to the manufacturers' protocol. Briefly, *Bt* colonies were taken up with a sterile micropipette tip and subsequently suspended in 0.5 ml phosphate-buffered saline (PBS) in a 2 ml sterilized Eppendorf tube. Following spinning for 10 min at 10,000 x *g* and discarding supernatant, the resultant pellet was resuspended in 500 µl of InstaGene Matrix (Bio-Rad). Then, the tube was placed in an incubator at 56°C for 30 min followed by boiling for 15 min. gDNA was released outside the cell into the supernatant after boiling in the resin and bound to the lysis products and PCR inhibitors. For *Bt* genotyping, the following forward and reverse primers were employed for the PCR reaction to amplify rDNA fragment: 52 -AGA GTT TGA TCM TGG CTC AG-32 and 52 -TAC GGY TAC CTT GTT ACG ACT T-32, respectively. A 30 µl PCR reaction with gDNA template (30 ng) was setup in a thermal cycler (Veriti, Applied Biosystems, USA) according to the following cycling program: initial denaturation for 5 min at 95°C; followed by 30 cycles: 60 s at 95°C, 60 s at 55°C, 60 s at 72°C. Finally, a 10 min final elongation step at 72°C was performed. PCR amplicons of approximately 1400 bp were separated by 2% agarose gel electrophoresis in 1x Tris-borate-EDTA (TBE) for 30 min. The ethidium bromide-stained gels were examined under UV light using a gel documentation system (UVITEC, UK). Purified PCR amplicons were utilized to setup sequencing reaction by use of BigDye Terminator v3.1 Cycle Sequencing Kit (Thermo Fisher Scientific, Waltham, MA, USA). DNA sequencing based on chain-terminating inhibitors[20] by use of the following forward and reverse primers, 52 -CCA GCA GCC GCG GTA ATA CG-32 and 52 -TAC CAG GGT ATC TAA

TCC-32, respectively, was conducted on Applied Biosystems (Foster City, CA, USA) DNA analyzer model Prism 3730XL to resolve and analyze rDNA amplicons.

Alignment of rDNA Sequences and phylogenetic analysis

Pairwise sequence alignment of the PCR amplicons of the *Bt* strain under investigation (HAU-145) was conducted with reference to the standard *Bti*-H14 (*Bacillus thuringiensis* israelensis de Barjac) using the MultAlin interface (http://multalin.toulouse.inra.fr/multalin/).[21] Obtained *16S* sequence of HAU-145 was inputted into the standard nucleotide BLAST-Blastn suite of NCBI to check for potential similarity/identity hits. The phylogenetic tree was created using Drawtree 3.696 software, a tree viewer tool available on the website www.phylogeny.fr/, which is based on the neighbor-joining method.

Separation of parasporal (PS) crystal inclusion proteins

The bacterial *Bt*-HAU-145 culture was prepared in 0.5 L Anderson medium[22] for a minimum of 48 h at 30°C. Then, the obtained culture medium was subjected to centrifugation at 6000 x *g* under cooling at 4°C for 10 min. The resulting pellet was rinsed twice with 1 M NaCl supplemented with Triton X-100 (0.01%). The resultant pellet was subsequently suspended in a Falcon tube (50 mL) containing PBS to enhance the hydrophobic interactions. Hexane was subsequently added to 10% of the aqueous suspension, followed by sonication for 10 min at 100 W and finally, the tube was centrifuged for 10 min at 6000 x *g*. While *Bt* spores were trapped in the organic (hexane) upper layer, cell debris remained in the lower aqueous layer. Then, the pellet enriched with parasporal crystals was resuspended in PBS, and the whole procedure was performed by adding hexane three times. Finally, the pellet was washed twice with cold distilled water.[22]

Protein quantification

The Bradford colorimetric method was employed to determine the protein concentration in the parasporal crystal samples based on the binding of protein molecules to Coomassie Brilliant Blue.[23] The absorbance (A) was recorded at λ_{595nm} using a BioTek microplate ELISA reader (Synergy HT). A standard curve was constructed using serially diluted bovine serum albumin concentrations, and A on the y-axis was plotted against the concentration on the x-axis. The unknown protein concentration (mg/ml) was calculated using a linear equation.

SDS-PAGE

Sodium dodecyl sulfate-polyacrylamide gel electrophoresis (SDS-PAGE) of PS samples was conducted on a Mini-PROTEAN Tetra Vertical Electrophoresis Cell (Bio-Rad Laboratories, Hercules, CA, USA) according to standard protocol.[24,25] PS proteins were solubilized, and the protein final concentration was adjusted to 200 µg/mL^{-1} in Na_2CO_3 buffer (50 mM, pH 10.5) supplemented with DTT a final concentration of 10 mM. Next, PS protoxins were proteolytically activated by use of trypsin at a protease/PS ratio of 1/10 at 37°C. The Laemmli sample buffer (2x) was freshly mixed with a reducing agent at a ratio 1/10 freshly before use.[25] Equal amounts of parasporal protein and sample buffer (1/1) were prepared and boiled for 10 min. The mixture was loaded into wells with 10% TGX Precast Gels (Bio-Rad Laboratories). Electrophoresis was performed in 1x Tris-glycine SDS running buffer for 60 min at 150 V. The determination of the molecular mass of individual protein bands was conducted with reference to protein marker II (AppliChem GmbH, Darmstadt, Germany), comprising standard proteins with a M.W. range of aprotinin-6.5 to myosin-200 kDa.

Western blotting of apoptotic marker proteins

MDA-MB-231 cells were subjected to the IC_{50} concentration (*i.e.*, 28 µg/ml) of trypsinized parasporal crystal proteins for 48 h. DMSO was used as a negative control. After cell collection, protein was extracted using an extraction buffer containing 50 mM Tris-HCl (pH 7.5), 1 mM PMSF, and 0.1% NP-40, together with a cocktail of protease inhibitors. A sterile plastic pestle was used to grind the cells, and the proteins were quantified.[26] The electrophoresed PS proteins were transferred from the gel to PVDF membrane utilizing Trans Blot Turbo Transfer System (Bio-Rad Laboratories), in a semi-dry and rapid fashion that

lasted for 3 min at 25 v. Mini PVDF membranes (0.2 µm pore size) were subsequently washed thrice with 1x PBS for 5 min followed by blocking with FBS with shaking for at least 1 h. PVDF membrane was incubated with primary anti-caspase-3 polyclonal (ab13847; Abcam, Cambridge, UK), anti-Bcl2 monoclonal (E17; ab32124; Abcam) and anti-β-Actin monoclonal (SP124; ab115777; Abcam) followed by secondary antibodies.[26] The chemiluminescent signals from the protein bands were detected by scanning the membrane using ChemiDoc XRS Imaging (Bio-Rad Laboratories).

Anti-proliferative MTT assay

Cytotoxicity in MDA-MB-231 cells was determined by measuring the absorbance of purple formazan resulting from the enzymatic reduction of yellow water-soluble MTT (3-(4,5-dimethylthiazol-2-yl)-2,5-diphenyltetrazolium bromide) tetrazolium dye, as previously reported. This is a 96-well microtiter plate assay whose absorption was measured by use of Bio-Tek microplate ELISA reader (Synergy HT, Winooski, Vermont, USA). Cellular metabolic activities represented by the absorbance (y-xis) at l 549 nm were graphically plotted against the concentration (x-axis) of trypsinized PS using the GraphPad Prism 9 software. The PS concentration that led to a 50 percent inhibition (IC_{50}) of cell proliferation was determined from the generated regression curves. Dasatinib, an effective multi-targeted kinase antagonist for BCR-ABL and SRC-related kinases,[27] was tested at the same doses as the evaluated PS proteins on MDA-MB-231 cells, serving as an established positive control for comparative assessment. Normal epithelial breast MCF-12 cells served as controls to evaluate selectivity.

Apoptosis detection by Annexin V staining

MDA-MB-231 cells were treated with the IC_{50} concentration (*i.e.*, 28 µg/ml) of trypsinized parasporal crystal proteins for 48 h. DMSO was used as a negative control. For flow cytometry, a Dead Cell Apoptosis Kit containing both Annexin V FITC and PI dyes (Thermo Fisher Scientific, Waltham, MA, USA) was used, as previously described.[28] Briefly, after cell collection by centrifugation at 3000 x *g* for 3 min, the pelleted cells were rinsed three times with PBS and centrifuged for 3 min at 3000 x *g*. 1x binding buffer was used to resuspend the cells at a density of $1x10^6$ cells. ml^{-1}. Cell suspension of 100µl was subsequently stained with 1µl of 1x Propidium Iodide (PI) and 5µl of Annexin V-FITC. The tubes were then placed in the dark at laboratory temperature for 20 min. Cells undergoing apoptosis were analyzed by use of Becton Dickinson flow cytometer model FACSCalibur (Franklin Lakes, NJ, USA). Annexin-V-FITC fluorescence was detected at $\lambda_{exc.}$ and $\lambda_{em.}$ at 488/520 and 535/670 nm, respectively.[17]

Oxidative stress detection by dichlorofluorescein staining

In order to monitor intracellular generation of reactive oxidative species (ROS) in PS-treated MCF-7 breast cancer cells, 22,72 -dichlorodihydrofluorescein diacetate (H2DCFDA; Thermo Fisher Scientific) was employed.[29] Following collection by spinning and washing with PBS, cells were labeled by H2DCFDA (10 µM) and placed in the dark at 37°C for 30 min. The fluorescence of the generated 22,72 -dichlorofluorescein (DCF) was measured $\lambda_{exc.}$ and $\lambda_{em.}$ of 488 nm at 520 nm, respectively by use of FACSCalibur (Becton Dickinson, Franklin Lakes, NJ, USA) flow cytometer.

Determination of caspase-3 enzymatic activity

Cancer cells at a concentration of $5×10^4$ were grown in TC-designated flasks and subsequently exposed for 48 h to the 1x (28 µg/ml), 5x (140 µg/ml) and 10x (280 µg/ml) of IC_{50} concentrations of *Bt*-derived PS that had been solubilized and trypsin-activated. DMSO at an equivalent dilution was used as a negative control. The enzymatic reaction was setup to accommodate the following components: 30 µl of either DMSO- or PS-treated cell lysate cancer cells, 20 µl of Ac-DEVDAFC as a substrate for caspase-3, 150 µl HEPES buffer at a concentration of 50 mM, EDTA (1 mM) and DTT (1 mM). After incubation at pH 7.2, the samples were measured $l_{ex.}$ at 430 nm and l_{em} at 535 nm on a Bio-Tek microplate ELISA reader (Synergy HT) over a period of 15 min at intervals of 5 min. The standard curve for the caspase-3 substrate AFC (7-amido-4- trifluoromethylcoumarin) was constructed with concentrations between 5 and 15 µM. The obtained fluorescence was transformed into caspase-3 enzyme activity after calculation

and was expressed in pM of enzymatically released AFC min^{-1}/mg^{-1} protein.[17]

Statistical analysis

Statistical analyses were performed using the Statistical Package for Social Sciences version 17.0 (SPSS; Armonk, NY, USA). Three independent experiments were conducted in duplicate. Calculated data were expressed in terms of mean ± SD. To verify significant differences between PS-treated and mock-treated vehicle (DMSO solvent) controls, data were analyzed using a paired Student's *t*-test. Mean values were considered statistically significant at $p < 0.05$.

RESULTS

Molecular typing of *Bt* HAU-145

The isolated HAU-14 bacterial strain native to the city of Hafr Al-Batin soil (GPS location: 28°12'30.1"N 45°55'30.1'E, KSA) was molecularly identified as *Bacillus thuringienesis* by *16S* rDNA sequencing as detailed in the methods section. Amplification of the *16S* rDNA gene using PCR was conducted on the isolated HAU-145 strain and the reference strain *Bti*-H14 (Figure 1). A PCR amplicon of the expected size of approximately 1400 bp was obtained.

A Blastn similarity/identity hit search of the *16S* rDNA sequence revealed a high similarity of 99% (E value = 0.0) with the rDNA gene sequence of the reference strain *Bti*-H14. This high similarity is clearly observed in the pairwise similarity diagram shown in Figure 2. Red bases indicate high similarity between the *16S* DNA of the reference strains *Bti*-H14 and HAU-145. This confirms that the strain under investigation belongs to the species *Bacillus thuringienesis*. Phylogenetic analysis was performed using the neighbor-joining method. The phylogenetic tree confirmed the high similarity of the *16S* rDNA sequence with several *B. thuringienesis* and *B. cereus* sequences (Figure 3).

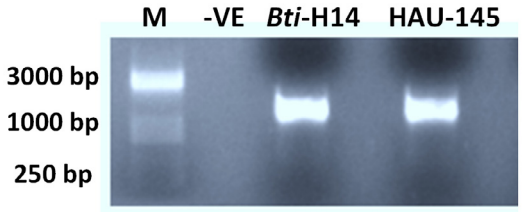

Figure 1. Agarose gel electrophoresis of *16S* rDNA PCR amplicons. M: DNA marker. -VE negative control. Products have size of around 1400 bp after having been electrophoresed for 30 min at 100 v in 2% agarose

Biochemical typing of *Bt* HAU-145

Discriminating test results of API 20E and API CH50 were used for the biochemical typing of strain *Bt* HAU-145. Notably, *Bt* HAU-145 strain was nonhemolytic (negative in the hemolysis test) and positive in the motility (MOT) test. Moreover, it exhibited distinctive positive phenotypes for amygdalin (AMY), citrate utilization (CIT), arginine decarboxylation (ADH) proteolytic activity of gelatinase (GEL), hydrolysis of both lecithin and esculin, L-tryptophan deaminase enzymes (TDA) as well as D-glucose (GLU) and sucrose (SAC) fermentation. In contrast, the strain was negative for D-sorbitol (SOR) fermentation, rhamnose (RHA), D-melibiose (MEL), the Voges Proskauer (VP) test, oxidase activity (OX), and salicin (SAL), hydrogen sulfide (H_2S), urease (URE), and indole (IND) production.

***Bt* HAU-145 possess spherical-shaped crystal parasporal proteins**

The morphological structure of the crystal-spore complexes of *Bt* HAU-145 was examined using phase-contrast and scanning electron microscopy (SEM) (Figure 4A and B). Microscopic examination revealed that parasporal crystals were attached to the spores and did not detach. Moreover, SEM examination revealed that the crystals were spherical (Figure 4B).

Visualization of protoxin and activated parasporal proteins by SDS-PAGE

SDS-PAGE was conducted to visualize the protein profile of purified parasporal proteins in both trypsin-activated and protoxin forms (Figure 5). Two distinct protein profiles were observed: unactivated (U) and activated (A). The unactivated parasporal protein profile contained two major bands of approximately 80 and 30 kDa. Moreover, four minor bands were visualized in the unactivated parasporal protein profile: two immediately below the major band at 80 kDa and two just above the 47 kDa marker band. In

contrast, the activated parasporal protein profile primarily contained a 30 kDa band.

Bt HAU-145-derived parasporal proteins exhibit selective anticancer activity against cells

The cytotoxic activity of activated (*i.e.*, trypsin-digested) parasporal crystals derived from *Bt* HAU-145 against MDA-MB-231 cells was determined using an MTT assay. The IC_{50} value for the activated parasporal crystal was calculated to be 28 µg/mL (Figure 6).

The cytotoxic effects showed a clear dose-dependent response. This observed cytotoxic effect was confined to cancerous cells, as the activated parasporal crystals exhibited significant cytotoxicity towards MDA-MB-231 cells but not against healthy MCF-12 breast control cells (less than 5%). Notably, the antiproliferative effect of the unactivated parasporal crystals was negligible towards normal epithelial breast MCF-12 cells, indicative of its selectivity.

Exposure of MDA-MB-231 cells to parasporins causes apoptosis

Analysis based on FACS flow cytometry using Annexin V- /Propidium Iodide dual labeling

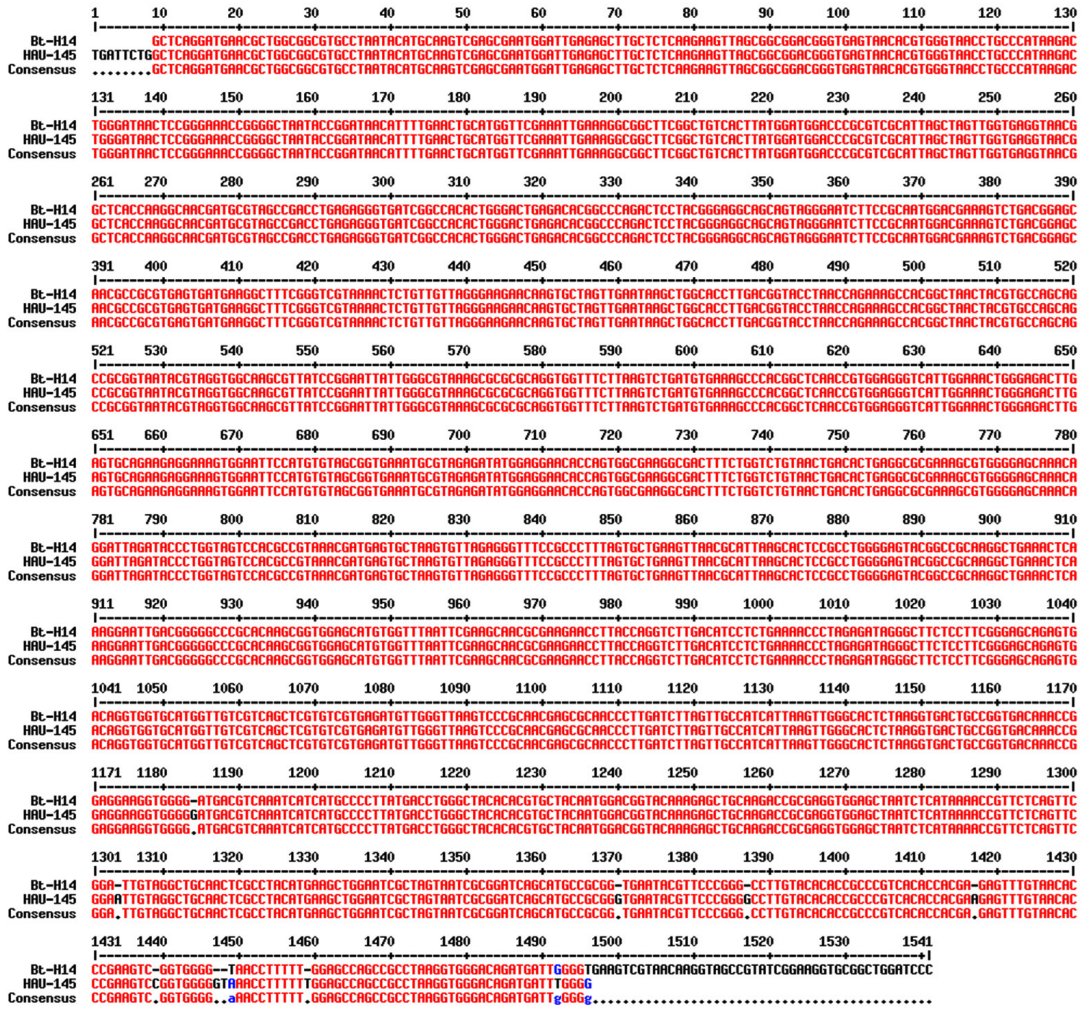

Figure 2. Sequence alignment of the *16S* rDNA of *Bt* HAU-145 with that of the reference *Bt*i-H14 strain. The pairwise alignment was carried out using MultiAlin interface.[24] Red color indicates identical bases, whereas blue color indicates non-identical or mismatched bases

was employed to ascertain whether the observed cytotoxicity of activated PS proteins against MDA-MB-231 cells was mediated through the induction of programmed cell death (*i.e.*, apoptosis). The results indicated that the exposure of breast cancer cells to PS proteins significantly triggered cells to undergo both early (top right quadrant) and late (bottom right quadrant) phases (Figure 7).

Exposure of MDA-MB-231 cells to parasporins causes oxidative stress

The involvement of reactive oxygen species (ROS) was investigated using the cell-permeable probe, H2DCFDA. Upon the generation of ROS, H2DCFDA is intracellularly oxidized to 22,72-dichlorofluorescein (DCF). Apoptotic PS-exposed MDA-MB-231 cells appeared to generate greater levels of ROS than DMSO-treated controls

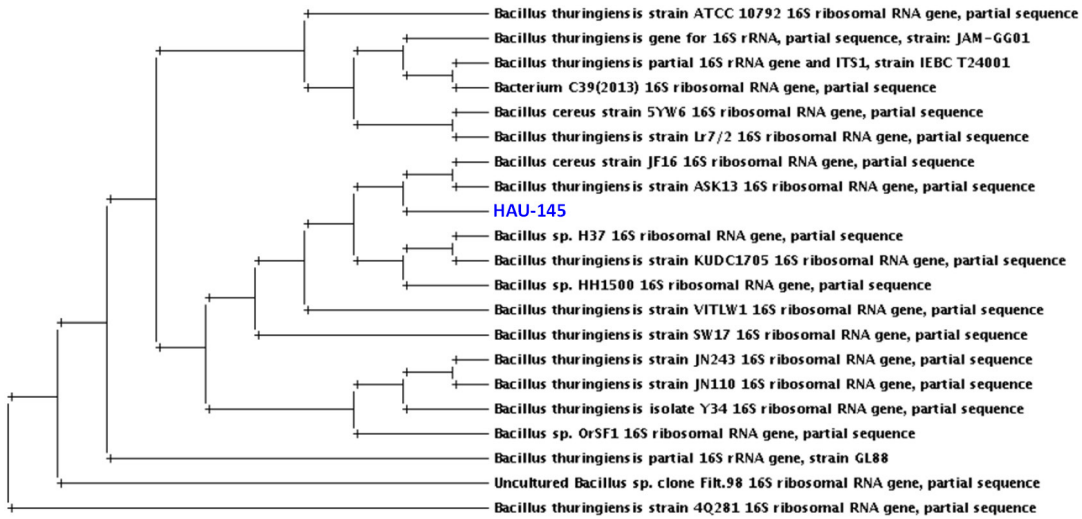

Figure 3. Phylogenetic analysis of *16s* rRNA of *Bt* HAU-145 strain compared with selected *Bt* and *B. cereus* strains whose sequences were obtained from GenBank®. The phylogenetic tree was created by use of Drawtree 3.696 software, which is one of the Tree viewers tools at www.phylogeny.fr/ base on the neighbor-joining method

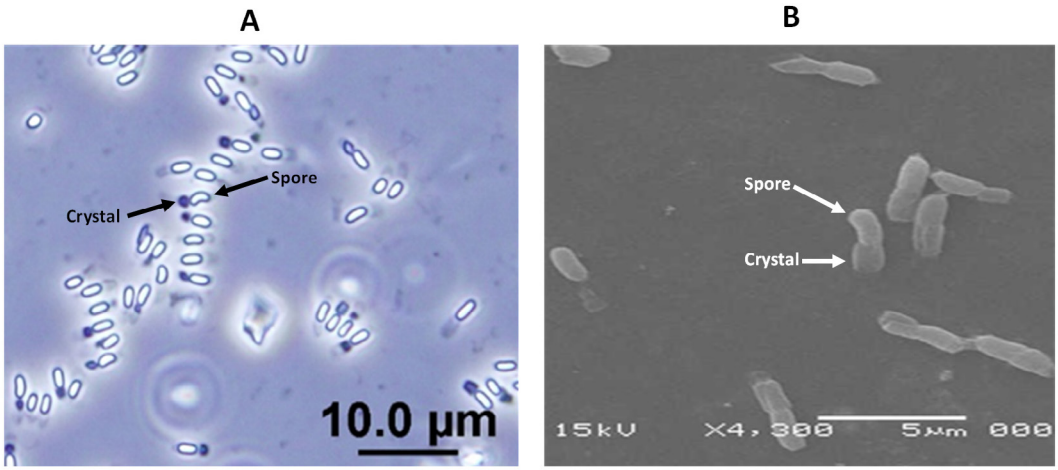

Figure 4. Micrographs of the native non-hemolytic *Bt* HAU-145 illustrating parasporal crystal-spore complexes taken by phase-contrast (A) and scanning electron microscopy. Black arrows point to spores and crystals. Scale bars annotate image size in µm

(Figure 8A and B). Specifically, PS-exposed cells elicited 29.4% ROS (Figure 8B), compared to only 2.6% ROS in the DMSO-treated control (Figure 8A).

Parasporins modulate the protein expression of apoptotic markers

Immunoblotting was conducted to investigate the modulatory potential of parasporins on the expression of two selected apoptotic marker proteins, the pro-apoptotic marker caspase-3 and the anti-apoptotic marker Bcl-2. Notably, profound induction in the expression of the pro-apoptotic "executioner" caspase-3 at 12 and 24 h post-exposure to the IC_{50} concentration of activated parasporin crystal proteins that have been isolated from *Bt* HAU-145 (Figure 9). In contrast, a notable reduction in the expression of Bcl-2, an anti-apoptotic marker, was observed at 12 and 24 h post-exposure to the IC_{50} concentration of activated parasporin crystal proteins isolated from *Bt* HAU-145 (Figure 9).

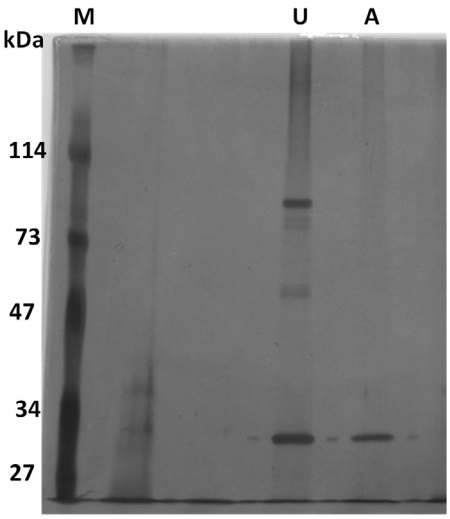

Figure 5. SDS-PAGE of *Bt* HAU-145 solubilized parasporal crystal proteins. U, unactivated. A, Activated (*i.e.*, trypsinized) inclusions. PS proteins were separated SDS-PAGE gel (10% TGX) and was subsequently subjected to by silver staining for band detection (Methods)

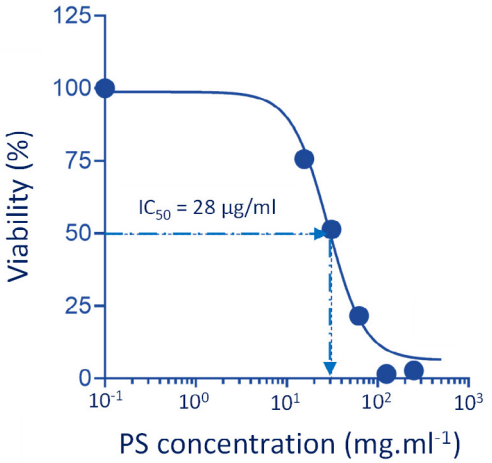

Figure 6. Effect of activated parasporal crystal proteins derived from Bt HAU-145 on MDA-MB231 cells

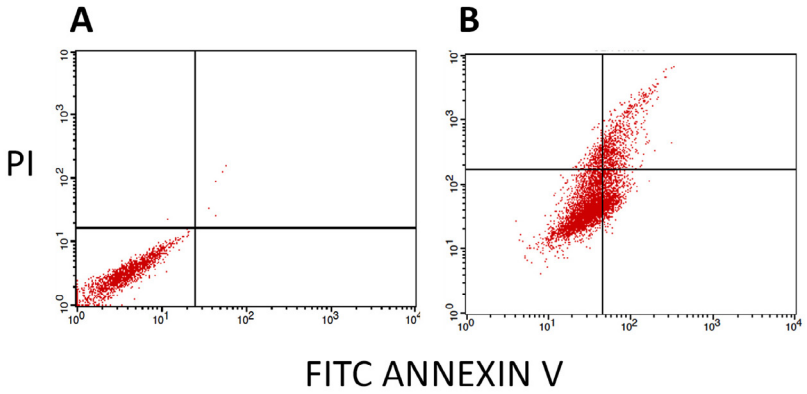

Figure 7. Annexin V-FITC/PI FACS assessment of the apoptosis-inducing capacity of activated parasporal proteins derived from *Bt* HAU-145 in MDA-MB-231. (A): FACS analysis of MDA-MB-231cells after 48 h treatment with DMSO (solvent control). (B): FACS analysis of MDA-MB-231cells after 48 h exposure to IC_{50} (28 µg/ml) concentration of trypsin-activated parasporal proteins. While the Y-axis represents the PI-labeled cell population, the X-axis indicates the FITC-labeled annexin V-positive cells

Parasporins upregulate enzymatic activity of caspase-3

Forty-eight-hour exposure of MDA-MB-231 cells to PS concentrations (*i.e.*, 28, 140, or 280 µg activated-PS/ml, which are equivalent to 1x, 5x, and 10x IC_{50}, significantly induced caspase-3 enzymatic activity compared to DMSO solvent control (Figure 10). The 1x and 5x IC_{50} concentrations of activated PS resulted in a clear upregulation of caspase-3 activity ($p < 0.05$). A more significant upregulation in the activity of caspase-3 was detected when MDA-MB-231 cells were exposed to 10x (68 µg/ml) IC_{50} concentration of activated-PS at significance p value < 0.01 (Figure 10).

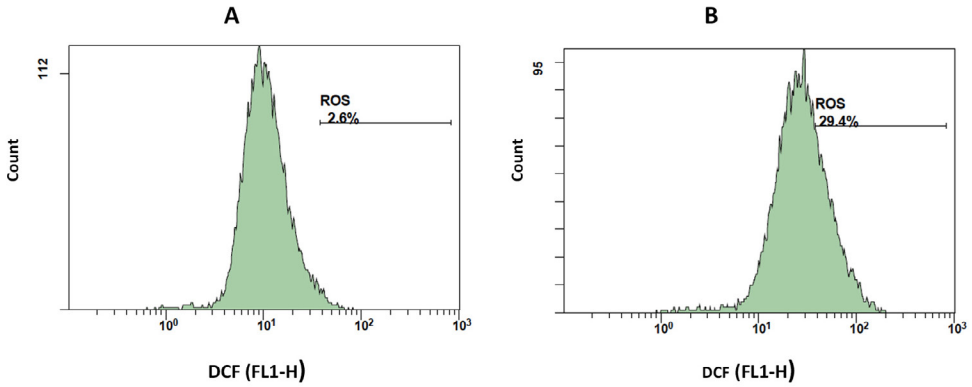

Figure 8. Activated parasporins induce oxidative stress in MDA-MB-231 cells. Histograms show DCF fluorescence intensity (FL1-H) versus cell counts depicting intracellular ROS outbreak in MDA-MB-231 cells after 48 h exposure to DMSO (A) and IC_{50} (28 µg/ml) concentration of parasporins (B)

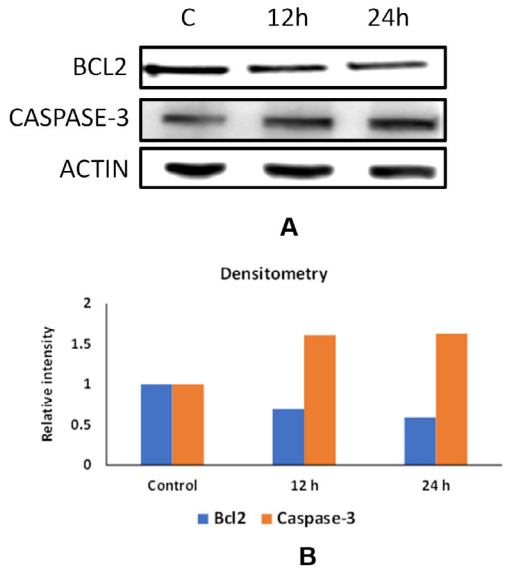

Figure 9. Effect of activated parasporins on the expression of apoptotic protein markers in MDA-MB-231 cells. (A) Immunoblotting of Bcl-2 and Caspase-3 proteins with reference to β-actin. (B) densitometric analysis of band intensities by use of ImageJ software (NIH). Adherent cells were exposed to 28 µg/mL concentration, which is equivalent to the IC_{50} concentration of activated parasporins for 12 and 24 h

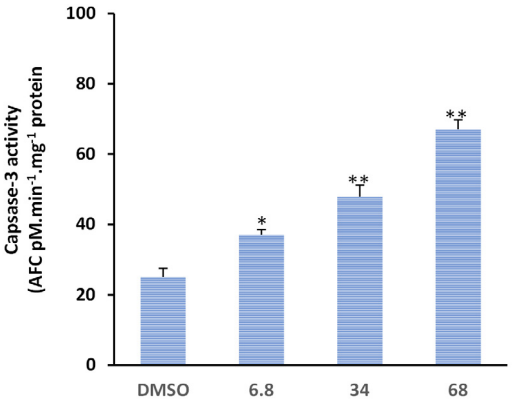

Figure 10. Activated parasporins induce caspase-3 enzymatic activity in MDA-MB-231 breast cancer cells. DMSO was used as solvent control. MDA-MB-231 cells were exposed for 48 h with increasing concentrations (1x, 28; 5x, 140 and 10x, 280 µg/ml) of activated PS proteins. *p<0.05, **p<0.01

DISCUSSION

In the present study, we examined the anticancer activity of a non-hemolytic native *Bacillus thuringiensis* (*Bt*) strain that had been isolated from the Hafr Al-Batin region in Saudi Arabia. The isolated strain was typed both biochemically and molecularly using API 20E, API CH50, and *16S* rDNA sequencing. Biochemical typing revealed that the isolated strain was non-hemolytic. The non-hemolytic feature of *Bt* strains has been attributed to the absence of Cty proteins.[30,31] The inability to induce hemolysis has been reported to be one of the two essential features, along with non-insecticidal activity, of *Bt* strains that produce anticancer PS proteins.[13,32] This observation was the driving motive to investigate the anticancer activity of *Bt* HAU-145 in the current study. However, before further characterization, it was important to verify the identity of the isolated strains. In this context, *16S* rDNA molecular typing was conducted to compare the sequences of standard *Bti*-H14 and *B. cereus* strains. Based on the Sanger sequencing data of the PCR amplicons, the strain under investigation, HAU-145 was confirmed to be a *Bt* strain (Figures 1, 2, and 3). The 99% homology to the reference *Bt*-H14 strain conforms to a previously published report on Saudi Arabian strains, which showed 99.5% homology.[18] Phase-contrast and SEM microscopic examinations revealed that *Bt* HAU-145 possessed a spherical parasporal crystal (Figure 4). Previously, it was reported that *Bt* isolates from different geographical regions worldwide exhibited variable crystal morphological features, including spherical, bi-pyramidal, or irregular shapes.[33-36] This finding confirms previous results on *Bt* strains of Saudi Arabian origin and highlights the diversity and variation in crystal protein morphology.[15,18]

SDS-PAGE revealed that the nascent (unactivated) parasporal protein profile contained two major bands at approximately 80 and 30 kDa. Upon activation, the major band at 80 kDa was completely lost, leaving only one band at approximately 30 kDa (Figure 5). Interestingly, it has been reported the *Bt* A1190 strain produces a nascent PS1Aa1 protein of 81 kDa. Proteolytic cleavage produced two protein bands at 56 and 15 kDa.[32] Therefore, it is plausible that the *Bt* HAU-145 strain produces a PS protein that resembles PS1. However, this possibility remains to be confirmed by sequencing its gene and protein. The fact that the 15 kDa band is completely missing from the SDS-PAGE profile of the activated PS protein from *Bt* HAU-145 remains to be reconciled.

MTT anti-proliferation assay revealed that the activated form of PS protein isolated from *Bt* HAU-14 exhibits potent cytotoxicity towards MDA-MB-231, which is classified as a triple negative breast cancer cell model, with an IC_{50} of 28 µg/ml (Figure 6). This finding is in agreement with our previous report on Saudi Arabian *Bt* non-insecticidal and non-hemolytic strains, which showed that they exhibit cytotoxicity against HeLa cells, a cervical cancer model. This cytotoxicity has been shown to be specific to cervical cancer cells, as no tangible effects were observed in colon cancer cells.[15] Previous reports have pointed to the wide cytotoxic spectrum of PS1 proteins, not only against cervical cancer cells but also against leukemic and hepatocarcinoma cells.[32] Structurally, PS1, PS3, and PS6 are classified as PS-type proteins with a three-domain structure. As such, they share a high resemblance to Cry toxins, as they also possess five-block domains.[32,37-39] To elucidate the mechanism of action of activated PS protein derived from *Bt* HAU-145 cells, immunoblotting and FACS analyses were conducted. Annexin-V/PI double staining revealed that the enhanced *Bt* HAU-145-mediated cytotoxic activity against MDA-MB-231 cells was mediated by both early and late apoptosis (Figure 7). This staining technique is since cells undergoing apoptosis translocate phosphatidylserine (PS) residues to the exterior of the plasma membrane. In this case, the exposed PS residues could be easily detected by staining with the fluorescent probe Annexin V, a protein molecule that exhibits potent affinity for PS. Later in the apoptotic process, cell membrane integrity is lost, thereby permitting the free diffusion of PI inside the cells and subsequent binding to DNA. Hence, high PI fluorescence indicated late apoptotic and necrotic cell death.[27] Moreover, FACS analysis clearly indicated that the activated PS protein derived from *Bt* HAU-145 cells induced significant oxidative stress (OS) in terms of ROS generation (Figure 8). Previous studies have shown a cause-and-effect association between aggravated generation of OS and ROS production from one side and the induction of

apoptosis. It is widely known that one of the main hallmarks of cancer progression is the ability to resist or overcome intracellular apoptotic cues.[40] Therefore, apoptosis is central to drug discovery as a target for cancer therapeutics.[10] In the event of malfunction in the antioxidant machinery that detoxifies and scavenges ROS, an outbreak of OS occurs, leading to a heightened risk of developing breast cancer. This is ascribed to the detrimental effects of ROS on biological molecules, such as nucleic acids, proteins, and lipids. This outbreak would eventually lead to inflammation, cell cycle arrest, apoptosis, and necrosis.[41,42] The FACS findings reported in the current study on the PS-mediated impact on the induction of apoptosis (Figure 7) were further confirmed by immunoblotting of two apoptotic markers (Figure 9). Western blotting revealed contrasting findings regarding the expression levels of two apoptotic markers, caspase-3 (pro-apoptotic) and Bcl-2 (anti-apoptotic). While the expression levels of caspase-3 were enhanced at 12 and 24 h post-treatment with activated PS proteins in MDA-MB-231 cells, Bcl-2 expression levels were significantly reduced (Figure 9). The enzymatic activity of caspase-3 has also been found to be enhanced in a dose-dependent manner, which further confirmed the immunoblotting results (Figure 10). Active caspase-3 is catalytically produced by the proteolysis of its zymogen precursor, procaspase-3. This in turn results in the production of an activated 'executioner' form of caspase that catalyzes the hydrolytic process of several protein substrates within the apoptosis cascade.[43] Collectively, these results clearly indicate that PS treatment resulted in the activation of the apoptotic pathway. Current literature on the mode of action of PS proteins is scarce, with only a limited number of studies reporting the enhancement of apoptosis. Among these, a recent study reported the isolation of PS A13-2 from a Mexican *Bt* strain that exhibited potent and selective cytotoxic activity against a triple-positive MCF-7 breast cancer cell line.[44] Moreover, PS A13-2 has been reported to exhibit an IC_{50} of 6 µg/ml, which is very similar to that reported in the current study by PS-derived from *Bt* HAU-145 (28 µg/ml). Notably, this study also reported that PS A13-2 was ineffective against two other types of breast cancer cells: MDA-MB-231 and MDA-MB-468.[44] This observation is intriguing and clearly highlights the uniqueness of the cytotoxicity of a given PS protein not only against a different type of cancer, but also against subtypes within the same cancer type. PS A13-2-mediated cytotoxicity against MCF-7 cells has been reported to be mediated through late apoptosis and necrosis[44] independent of ROS generation, which conflicts with our findings. This can be explained by a difference in the molecular structure of the two types of PS proteins in the two reports, and therefore, differences in the downstream molecular targets and cascades. Moreover, this might imply that some PS proteins induce apoptosis through a ROS-independent mechanism, which requires further investigation.

CONCLUSION

PS proteins derived from the *Bt* HAU-145 strain are under investigation for their selective cytotoxicity against the triple-negative breast cancer cell line MDA-MB-231. The cytotoxic effect has been shown to be associated with apoptosis induction that proceeds through a ROS-dependent mechanism. Further investigation is warranted to dissect the molecular structure of the PS protein and its downstream targets. Moreover, it is necessary to test *in vivo* anticancer effectiveness of the PS proteins derived from *Bt* HAU-145 in preclinical experiments with non-human primates.

ACKNOWLEDGMENTS

None.

CONFLICT OF INTEREST

The authors declare that there is no conflict of interest.

AUTHORS' CONTRIBUTION

TAE conceptualized and designed the study. MMA collected resources. MMA and MAMA applied methodology. MMA and TAE performed formal analysis. MMA and MAMA performed investigation. TAE validated the data. MAMA performed visualization. MMA and MAMA wrote the original draft. TAE and MAMA wrote, reviewed, edited the manuscript and performed supervision. All authors read and approved the final manuscript for publication.

FUNDING

None.

DATA AVAILABILITY

All datasets generated or analyzed during this study are included in the manuscript.

ETHICS STATEMENT

Not applibale.

REFERENCES

1. IARC. The International Agency for Research on Cancer (IARC), Global Cancer Observatory, World Health Organization (WHO). Report on the Latest Estimates on the Global Burden of Cancer. Date of Release: 12 September 2018 in Geneva, Switzerland. Available online: https://www.iarc.fr/wp-content/uploads/2018/09/pr263_E.pdf (accessed on 22 May 2023). 2018.
2. IARC-WHO. Globocan. Saudi Arabia Source: Globocan Incidence, Mortality and Prevalence by cancer site. Available online at: https://gco.iarc.fr/today/data/factsheets/populations/682-saudi-arabia-fact-sheets.pdf(accessed on 22 May 2023). IARC 2020:1–2.
3. Alqahtani WS, Almufareh NA, Domiaty DM, et al. Epidemiology of cancer in Saudi Arabia thru 2010–2019: a systematic review with constrained meta-analysis. AIMS Public Health 2020;7:679. doi: 10.3934/PUBLICHEALTH.2020053
4. Chavez KJ, Garimella S V., Lipkowitz S. Triple negative breast cancer cell lines: one tool in the search for better treatment of triple negative breast cancer. *Breast Dis.* 2010;32:35–48. doi: 10.3233/BD-2010-0307
5. Xie X, Lee J, Liu H, et al. Birinapant Enhances Gemcitabine's Antitumor Efficacy in Triple-Negative Breast Cancer by Inducing Intrinsic Pathway-Dependent Apoptosis. Mol Cancer Ther 2021;20:296–306. doi: 10.1158/1535-7163.MCT-19-1160.
6. Aboul-Soud MAM, Ashour AE, Challis JK, et al. Biochemical and molecular investigation of in vitro antioxidant and anticancer activity spectrum of crude extracts of willow leaves salix safsaf. Plants 2020;9. https://doi.org/10.3390/plants9101295.
7. Aboul-Soud MAM, El-Shemy HA, Aboul-Enein KM, Mahmoud AM, Al-Abd AM, Lightfoot DA. Effects of plant-derived anti-leukemic drugs on individualized leukemic cell population profiles in Egyptian patients. Oncol Lett 2016;11:642–8. doi: 10.3892/ol.2015.3916.
8. Mahmoud AM, Aboul-Soud MAM, Han J, Al-Sheikh YA, Al-Abd AM, El-Shemy HA. Transcriptional profiling of breast cancer cells in response to mevinolin: Evidence of cell cycle arrest, DNA degradation and apoptosis. Int J Oncol 2016;48:1886–94. doi: 10.3892/ijo.2016.3418.
9. El-Shemy H, Aboul-Soud M, Nassr-Allah A, Aboul-Enein K, Kabash A, Yagi A. Antitumor Properties and Modulation of Antioxidant Enzymes Activity by Aloe vera Leaf Active Principles Isolated via Supercritical Carbon Dioxide Extraction. Curr Med Chem 2009;17:129–38. doi: 10.2174/092986710790112620.
10. Ashour AE, Ahmed AF, Kumar A, Zoheir KMA, Aboul-Soud MA, Ahmad SF, et al. Thymoquinone inhibits growth of human medulloblastoma cells by inducing oxidative stress and caspase-dependent apoptosis while suppressing NF-κB signaling and IL-8 expression. Mol Cell Biochem 2016;416:141–55. doi: 10.1007/S11010-016-2703-4
11. Zhang Y, Wang C, Zhang W, Li X. Bioactive peptides for anticancer therapies. Biomaterials Translational 2023;4:5. doi: 10.12336/BIOMATERTRANSL.2023.01.003
12. Ahmad I, Pal S, Singh R, Ahmad K, Dey N, Srivastava A, et al. Antimicrobial peptide moricin induces ROS mediated caspase-dependent apoptosis in human triple-negative breast cancer via suppression of notch pathway. Cancer Cell Int 2023;23:1–17. doi: 10.1186/S12935-023-02958-Y/FIGURES/8
13. Mizuki E, Park YS, Saitoh H, Yamashita S, Akao T, Higuchi K, et al. Parasporin, a Human Leukemic Cell-Recognizing Parasporal Protein of Bacillus thuringiensis. Clin Diagn Lab Immunol 2000;7:625. doi: 10.1128/CDLI.7.4.625-634.2000
14. Mizuki E, Ohba M, Akao T, Yamashita S, Saitoh H, Park YS. Unique activity associated with non-insecticidal Bacillus thuringiensis parasporal inclusions: In vitro cell-killing action on human cancer cells. J Appl Microbiol 1999;86:477–86. doi: 10.1046/J.1365-2672.1999.00692.X/PDF.
15. Aboul-Soud MAM, Al-Amri MZ, Kumar A, Al-Sheikh YA, Ashour AE, El-Kersh TA. Specific Cytotoxic Effects of Parasporal Crystal Proteins Isolated from Native Saudi Arabian Bacillus thuringiensis Strains against Cervical Cancer Cells. Molecules 2019, Vol 24, Page 506 2019;24:506. doi: 10.3390/MOLECULES24030506
16. Assaeedi AS, Osman GH. Screening and identification of Bacillus thuringiensis strains native to Saudi Arabia that exhibit demonstrable anticancer activity. *J Pure Appl Microbiol.*2017;11(1):119–128. doi: 10.22207/JPAM.11.1.16
17. Aboul-Soud MAM, Ennaji H, Kumar A, Alfhili MA, Bari A, Ahamed M, et al. Antioxidant, Anti-Proliferative Activity and Chemical Fingerprinting of Centaurea calcitrapa against Breast Cancer Cells and Molecular Docking of Caspase-3. Antioxidants 2022, Vol 11, Page 1514 2022;11:1514. doi: 10.3390/ANTIOX11081514
18. El-Kersh TA, Ahmed AM, Al-Sheikh YA, Tripet F, Ibrahim MS, Metwalli AAM. Isolation and characterization of native Bacillus thuringiensis strains from Saudi Arabia with enhanced larvicidal toxicity against the mosquito vector Anopheles gambiae (s.l.). Parasit Vectors 2016;9. doi: 10.1186/S13071-016-1922-6
19. Logan NA, Berkeley RCW. Identification of Bacillus strains using the API system. J Gen Microbiol 1984;130:1871–82. doi: 10.1099/00221287-130-7-1871
20. Sanger F, Nicklen S, Coulson AR. DNA sequencing with chain-terminating inhibitors. Proc Natl Acad Sci U S A 1977;74:5463. doi: 10.1073/PNAS.74.12.5463
21. Corpet F. Multiple sequence alignment with hierarchical clustering. Nucleic Acids Res 1988;16:10881–90. doi: 10.1093/NAR/16.22.10881

22. Mounsef JR, Salameh D, Awad M kallassy, Chamy L, Brandam C, Lteif R. A simple method for the separation of Bacillus thuringiensis spores and crystals. J Microbiol Methods 2014;107:147–9. doi: 10.1016/J.MIMET.2014.10.003
23. Bradford M. A rapid and sensitive method for the quantitation of microgram quantities of protein utilizing the principle of protein-dye binding. Anal Biochem 1976;72:248–54. doi: 10.1006/ABIO.1976.9999.
24. Sambrook J, Fritsch EF, Maniatis T. Molecular cloning: a laboratory model 1989:xxxviii–1546.
25. Laemmli UK. Cleavage of Structural Proteins during the Assembly of the Head of Bacteriophage T4. Nature 1970 227:5259 1970;227:680–5. doi: 10.1038/227680a0.
26. Alzahrani AJ. Potent antioxidant and anticancer activities of the methanolic extract of Calligonum comosum (L'Her) fruit hairs against human hepatocarcinoma cells. Saudi J Biol Sci 2021;28:5283. doi: 10.1016/J.SJBS.2021.05.053
27. Ashour AE, Ahmed AF, Kumar A, Zoheir KMA, Aboul-Soud MA, Ahmad SF, et al. Thymoquinone inhibits growth of human medulloblastoma cells by inducing oxidative stress and caspase-dependent apoptosis while suppressing NF-κB signaling and IL-8 expression. Mol Cell Biochem 2016;416. doi: 10.1007/s11010-016-2703-4
28. Chen Z, Zhang B, Gao F, Shi R. Modulation of G2/M cell cycle arrest and apoptosis by luteolin in human colon cancer cells and xenografts. Oncol Lett 2018;15:1559. doi: 10.3892/OL.2017.7475
29. Kumar A, Alfhili MA, Bari A, Ennaji H, Ahamed M, Bourhia M, et al. Apoptosis-mediated anti-proliferative activity of Calligonum comosum against human breast cancer cells, and molecular docking of its major polyphenolics to Caspase-3. Front Cell Dev Biol 2022;10:2009. doi: 10.3389/FCELL.2022.972111/BIBTEX
30. Crickmore N, Zeigler DR, Feitelson J, Schnepf E, Van Rie J, Lereclus D, et al. Revision of the nomenclature for the Bacillus thuringiensis pesticidal crystal proteins. Microbiol Mol Biol Rev 1998;62:807–13. doi: 10.1128/MMBR.62.3.807-813.1998
31. Bravo A, Likitvivatanavong S, Gill SS, Soberón M. Bacillus thuringiensis: A story of a successful bioinsecticide. Insect Biochem Mol Biol 2011;41:423–31. doi: 10.1016/J.IBMB.2011.02.006
32. Katayama H, Yokota H, Akao T, Nakamura O, Ohba M, Mekada E, et al. Parasporin-1, a novel cytotoxic protein to human cells from non-insecticidal parasporal inclusions of Bacillus thuringiensis. J Biochem 2005;137:17–25. doi: 10.1093/JB/MVI003
33. Martin PAW, Gundersen-Rindal DE, Blackburn MB. Distribution of phenotypes among Bacillus thuringiensis strains. Syst Appl Microbiol 2010;33:204–8. doi: 10.1016/J.SYAPM.2010.04.002
34. Ito A, Sasaguri Y, Kitada S, Kusaka Y, Kuwano K, Masutomi K, et al. A Bacillus thuringiensis crystal protein with selective cytocidal action to human cells. J Biol Chem 2004;279:21282–6. doi: 10.1074/JBC.M401881200
35. Schnepf E, Crickmore N, Van Rie J, Lereclus D, Baum J, Feitelson J, et al. Bacillus thuringiensis and its pesticidal crystal proteins. Microbiol Mol Biol Rev 1998;62:775–806. doi: 10.1128/MMBR.62.3.775-806.1998
36. Ibarra JE, Del Rincón MC, Ordúz S, Noriega D, Benintende G, Monnerat R, et al. Diversity of Bacillus thuringiensis strains from Latin America with insecticidal activity against different mosquito species. Appl Environ Microbiol 2003;69:5269–74. doi: 10.1128/AEM.69.9.5269-5274.2003
37. Yamashita S, Katayama H, Saitoh H, Akao T, Park YS, Mizuki E, et al. Typical three-domain cry proteins of Bacillus thuringiensis strain A1462 exhibit cytocidal activity on limited human cancer cells. J Biochem 2005;138:663–72. doi: 10.1093/JB/MVI177
38. Nagamatsu Y, Okamura S, Saitou H, Akao T, Mizuki E. Three Cry toxins in two types from Bacillus thuringiensis strain M019 preferentially kill human hepatocyte cancer and uterus cervix cancer cells. Biosci Biotechnol Biochem 2010;74:494–8. doi: 10.1271/BBB.90615
39. De Maagd RA, Bravo A, Berry C, Crickmore N, Schnepf HE. Structure, diversity, and evolution of protein toxins from spore-forming entomopathogenic bacteria. Annu Rev Genet 2003;37:409–33. doi: 10.1146/ANNUREV.GENET.37.110801.143042
40. Hanahan D, Weinberg RA. The hallmarks of cancer. Cell 2000;100:57–70. doi: 10.1016/S0092-8674(00)81683-9.
41. Lee J, Giordano S, Zhang J. Autophagy, mitochondria and oxidative stress: cross-talk and redox signalling. Biochem J 2012;441:523–40. doi: 10.1042/BJ20111451
42. Galadari S, Rahman A, Pallichankandy S, Thayyullathil F. Reactive oxygen species and cancer paradox: To promote or to suppress? Free Radic Biol Med 2017;104:144–64. doi: 10.1016/J.FREERADBIOMED.2017.01.004
43. Boatright KM, Salvesen GS. Mechanisms of caspase activation. Curr Opin Cell Biol 2003;15:725–31. doi: 10.1016/j.ceb.2003.10.009
44. Borin DB, Castrejón-Arroyo K, Cruz-Nolasco A, Peña-Rico M, Rorato MS, Santos RCV, et al. Parasporin A13-2 of Bacillus thuringiensis Isolates from the Papaloapan Region (Mexico) Induce a Cytotoxic Effect by Late Apoptosis against Breast Cancer Cells. Toxins (Basel) 2021;13. doi: 10.3390/TOXINS13070476